Dynamic performance of a point absorber WEC considering nonlinear hardening spring under irregular waves

Zongyu Chang, Zhenhua Hou, and Zhongqiang Zheng

Abstract—**Wave energy is a kind of clean renewable energy that is huge and still need further research. Point absorber wave energy converter (PA-WEC) is widely utilized for offshore power devices. The PA-WEC utilizes the heave motion to drive linear electric generator or a hydraulic motor to generator using power take off (PTO) system. And the PTO system usually is assumed to be a linear spring and a linear damper. Because of the larger motion, the PTO system, which exhibited non-linear behavior, is considered as linear spring with the nonlinear hardening spring and a linear damper. Through the time domain method, the dynamic model of the PA-WEC is developed under irregular waves. The state space model replaced the convolution term in the frequency domain equation. The dynamic response of the PA-WEC is researched considering different environmental parameters by Runge-Kutta method. Then the power and power ratio performance of the system is obtained. Compare with the linear WEC, the results show that the nonlinear WEC can increase the power captured in irregular waves.**

Keywords—**wave energy converter, nonlinear hardening spring, PTO, irregular waves, state space model, dynamic performance**

I. INTRODUCTION

With the global climate change, the renewable energy is getting more and more attention. Wave energy is substantial as a clean renewable energy, and many WECs have been designed and analysed. The PA-WEC is widely utilized the depth of between 40 and 100 meters [1], and possesses very small dimensions relative to the incident wavelength [2]. So the effect of wave direction is not important for the capture of these devices, and can adapt to the various complex sea conditions.

Generally, the PTO system of WEC can be assumed as a linear spring and a linear damper in heave motion [3]. For this problem, many researchers have carried out. Crozier et al. [4] developed a heaving buoy for WEC using the coupled electromechanical and hydrodynamic simulation of a novel generator. Bailey and Bryden [5] assumed the PTO system including linear and nonlinear components due to the large amplitude to obtain the more accurate results. Zhang and Yang [6] debated the power capture performance of an oscillating-body WEC under irregular waves considering the nonlinear snap through PTO system. Tarrant and Meskell [7] described the dynamic stability of point absorbers in time-domain nonlinear numerical model. Manna and Sims [8] used the magnetic levitation to design a duffing oscillator to harvest energy. Pellegrini et al. [9] used nonlinear springs to harvest the energy in order to obtain the wide frequency band tuning. Liu [10] developed the duffing type nonlinear oscillator dynamic differential equation of wave energy conversion and found the large displacement excitation amplitude and nonlinear stiffness will increase the nonlinearity, output voltage and harvesting frequency bandwidth. Wilson et al. [11] demonstrated the performance of nonlinear WEC using the nonlinear cubic hardening spring and solved the dynamic response considering the nonlinear control. Sun et al. [12] used the finite element analysis software COMSOL Multiphysics to obtain the nonlinear hardening spring characteristic of magnetic. Wilson et al. [13] extended the concept of Complex Conjugate Control (CCC) to nonlinear WECs using Hamiltonian Surface Shaping and Power Flow Control (HSSPFC) to design the optimal limit cycles. Wu et al. [14] studied the nonlinear behavior of wave energy harvesting considering nonlinear stiffness in regular waves. Dang et al. [15] debated the WEC performance considering the variable stiffness mechanism (VSM). Zheng et al. [16] analyzed the dynamic response of the PA-WEC considering nonlinear hardening spring PTO systems with regular waves. Furthermore, the power capture of WEC

Manuscript received 13 April; accepted 8 December 2022; published 31 March 2023.

This work was supported in part by the National Natural Science Foundation of China (Grant No. 51809245 and 51875540).”

Zongyu Chang is with College of Engineering, Ocean University of China, Qingdao, China, 266100 (e-mail: zongyuchang@ouc.edu.cn).

Zhenhua Hou is with College of Engineering, Ocean University of China, Qingdao, China, 266100 (e-mail: 17862703693@163.com).

Zhongqiang Zheng is with College of Engineering, Ocean University of China, Qingdao, China, 266100 (e-mail: zqzheng@ouc.edu.cn).

Digital Object Identifier: https://doi.org/10.36688/imej.6.19-25

can be enhanced by different control strategies taking advantage of in PTO system, such as passive loading control [17], Latching Control [18], Reactive Loading Control [19], declutching control [20], model predictive control [21], near-optimal control [22], nonlinear model predictive control [23] and so on.

The WECs system is debated to maximize power absorption with large motion considering the nonlinear dynamic. So in this paper, the linear spring of PTO system is replaced by linear spring and nonlinear cubic hardening spring to obtain more accurate results with the PTO system generates power following floating motion. The motion model of the PA-WEC is developed in irregular waves using time domain method. The state space model replaced the convolution term in the frequency domain dynamic equation. The dynamic response of the PA-WEC is researched considering different environmental parameters by Runge-Kutta method. Then the power and power ratio performance of the system is obtained..

II. DYNAMIC MODEL OF POINT ABSORBER WEC UNDER IRREGULAR WAVES

A. JONSWAP spectrum

Generally speaking, the real sea state is defined by the wave spectrum. The JONSWAP spectrum [24] is used in this simulation.

$$S_\eta(\omega) = \alpha^* H_s^2 \frac{\omega_m^4}{\omega^5} exp\left[-\frac{5}{4}\left(\frac{\omega_m}{\omega}\right)^4\right] \gamma^{exp\left[-\frac{(\omega-\omega_m)^2}{2\sigma^2\omega_m^2}\right]} \quad (1)$$

where, $S_\eta(\omega)$ is the spectrum density function, ω is the circular frequency, H_s is the significant wave height, ω_m is the peak frequency, γ is the peak lifting factor. σ is the peak shape factor, and the value is

$$\sigma = \begin{cases} 0.09 & for \omega \geq \omega_m \\ 0.07 & for \omega < \omega_m \end{cases} \quad (2)$$

α^* is a coefficient related to γ as following:

$$\alpha^* = \frac{0.0624}{0.23 + 0.0336\gamma - 0.185\ (1.9+\gamma)^{-1}} \quad (3)$$

For times series calculation under irregular waves, the wave can be represented by series linear combination of sinusoidal waves.

$$\eta(t) = \sum_{i=1}^{N} \sqrt{2S_\eta(\omega_i)\Delta\omega}\, cos(\omega_i t + \varphi_i) \quad (4)$$

$\eta(t)$ is wave elevation; $\Delta\omega$ is small circular frequency interval; φ_i is random phase angle.

B. Dynamic model

For the larger motion, the nonlinear hardening spring is considered in simplified model of point absorber WEC as shown in Figure 1. And the system can be looked upon as a mass-damping-spring model. The motion of floating only is along with heave motion under the wave exciting force. In this paper, the motion of PTO system accompanies by the motion of the cylinder floating. The mass of the floating is $m = \rho\pi R^2 d_f$ (ρ is the density of seawater, R is radius of floating, d_f is the draft of floating).

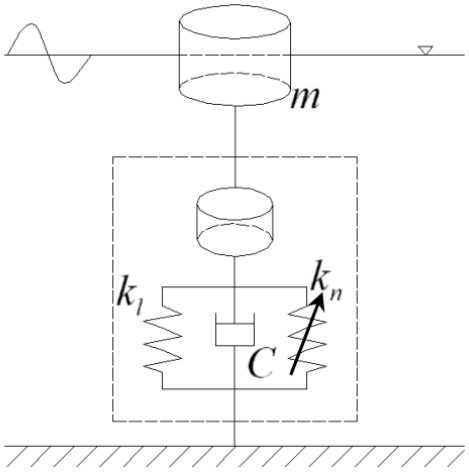

Fig. 1. PA-WEC with nonlinear hardening spring PTO system.

For this system, the time domain method [25] is applied to develop the dynamic model under irregular waves. In this paper, only considering the heave motion, the equation model of the PA-WEC system can be got as following:

$$[m + A_z(\infty)]\ddot{z}(t) + \int_0^t k_z(t-\tau)\dot{z}(t)d\tau + C\dot{z}(t) + \rho g S z(t) + k_l z(t) + k_n z^3(t) = F_{dzregular} \quad (5)$$

If $k_n = 0$, the system becomes linear PA-WEC as following

$$[m + A_z(\infty)]\ddot{z}(t) + \int_0^t k_z(t-\tau)\dot{z}(t)d\tau + C\dot{z}(t) + \rho g S z(t) + k_l z(t) = F_{dzregular} \quad (6)$$

where, z, $\dot{z}$, $\ddot{z}$ are the displacement, velocity and acceleration of the system in heave motion, $A_z(\infty)$is the added mass of the floating as $\omega = \infty$; $F_{dzregular}$ is the wave excitation force of the floating; S is the cross-sectional area of the floating and $S = \pi R^2$; C is the equivalent damping coefficient; k_l is the equivalent linear stiffness coefficient; k_n is the nonlinear hardening stiffness coefficient; $k_z(t)$, which is the retardation function, can be solved:

$$k_z(t) = \frac{2}{\pi}\int_0^\infty B_z(\omega)\, cos(\omega t) d\omega \quad (7)$$

where, $B_z(\omega)$ is the radiation damping coefficient of the floating in heave direction.

The module of wave excitation force $|F_{dzregular}|$ is

$$|F_{dzregular}| = \sum_{i=1}^{N} \Gamma_z(\omega_i) A_{\omega i} = \sum_{i=1}^{N} \Gamma_z(\omega_i) \sqrt{2 S_\eta(\omega_i) \Delta\omega} \tag{8}$$

where, $\Gamma_z(\omega_i)$ is the excitation force coefficient of floating in heave direction..

The parameters of the system are listed in TABLE I. Vicente, Falcão, and Justino [3] show that when the value of equivalent linear stiffness is $k_l = 0.1\rho g S$, the PTO system can obtained the most power. Using the AQWA software, the hydrodynamic coefficients of floating are calculated in heave direction as shown in Figure 2.

TABLE I
PARAMETERS OF THE SYSTEM

Symbol	Quantity	Unit
R	5	m
ρ	1025	kg·m^{-3}
d_f	3	m
k_l	$0.1\rho g S$	m/s

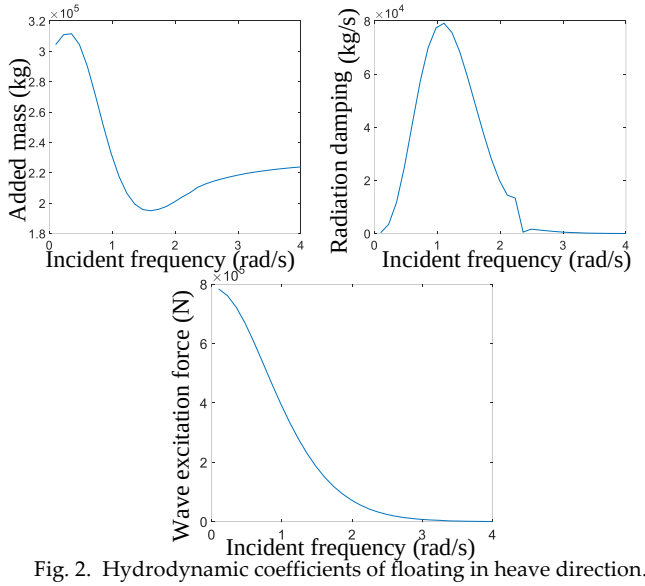

Fig. 2. Hydrodynamic coefficients of floating in heave direction.

Using the MATLAB curve fitting for polynomials, the wave excitation force coefficient $\Gamma_z(\omega)$ can be got as following

$$\Gamma_z(\omega) = -3269\omega^6 + 5.104\times10^4\omega^5 - 3.141\times10^5\omega^4 + 9.343\times10^5\omega^3 - 1.235\times10^6\omega^2 + 1.806\times10^5\omega + 7.761\times10^5 \tag{9}$$

In the frequency domain, the dynamic model of the system (6) can be written as

$$[m + A_z(\infty)]\ddot{z} + B_z(\omega)\dot{z} + \rho g S z = F_{dzregular} - C\dot{z} - k_l z \tag{10}$$

Using the complex amplitude z and $F_{dzregular}$. The function (10) can be solved

$$Z = \frac{f_{dzregular}}{-\omega^2[m + A_z(\omega)] + \rho g S + k_l + i\omega[B_z(\omega) + C]} \tag{11}$$

The power capture of WEC can be expressed as:

$$P = \frac{1}{2} C\omega^2 |Z|^2 = \frac{1}{8B_z(\omega)} \left|f_{dzregular}\right|^2 - \frac{B_z(\omega)}{2} \left|U - \frac{f_{dzregular}}{2B_z(\omega)}\right|^2 \tag{12}$$

where, U is the complex amplitude of velocity in the heave direction. For the power capture of WEC can get the maximum value, the function (12) need $U = \frac{f_{dzregular}}{(2B_z)}$. So, we can get as following

$$\omega = \left[\frac{\rho g S + k_l}{m + A_z(\omega)}\right]^{1/2} \tag{13}$$

$$C = B_z(\omega) \tag{14}$$

III. STATE SPACE MODEL

In this paper, the state-space model [16] [26] is used to instead of the From Figs. 3 and 4, the matrixes $\mathbf{A}'$,$\mathbf{B}'$, $\mathbf{C}'$ can be got convolution terms for dynamic solution. The typical state-space model usually can be expressed as

$$\begin{cases} \dot{\mathbf{X}}(t) = \mathbf{A}'\mathbf{X}(t) + \mathbf{B}'\dot{z}(t) \\ I_z(t) = \mathbf{C}'\mathbf{X}(t) \end{cases} \tag{15}$$

where, $I_z(t) = \int_0^t k_z(t-\tau)\dot{z}(t)d\tau$is the radiation force.

The MSS FDI Toolbox [27] is adopted for obtain the matrices $\mathbf{A}'$,$\mathbf{B}'$, $\mathbf{C}'$. According to the research data [16], $n = 5$ is selected as iteration number. The best identification results can be obtained as shown in Figures 3 and 4.

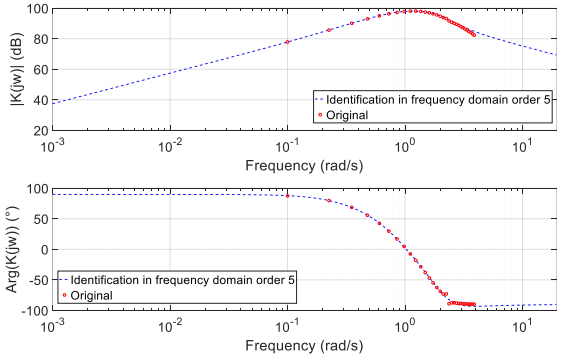

Fig. 3. The best identification results of the retardation function.

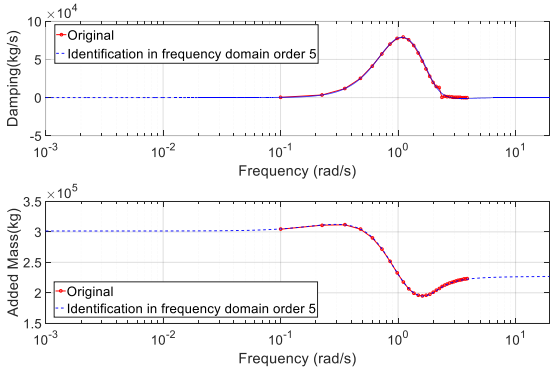

Fig. 4. The best identification results of the hydrodynamic coefficients

From Figs. 3 and 4, the matrixes $\mathbf{A}^{'}$,$\mathbf{B}^{'}$, $\mathbf{C}^{'}$ can be got

$$\mathbf{A}^{'}=\begin{bmatrix}-3.3213 & -7.6454 & -8.2999 & -5.1180 & -0.8772\\ 1 & 0 & 0 & 0 & 0\\ 0 & 1 & 0 & 0 & 0\\ 0 & 0 & 1 & 0 & 0\\ 0 & 0 & 0 & 1 & 0\end{bmatrix}$$

$$\mathbf{B}^{'}=\begin{bmatrix}1\\0\\0\\\vdots\\0\end{bmatrix}$$

$$\mathbf{C}^{'}=[56770 \quad 199640 \quad 371110 \quad 65454 \quad 0]$$

So, (5) and (6) can be written as following

$$[m+A_z(\infty)]\ddot{z}(t)+\mathbf{C}^{'}\mathbf{X}(t)+C\dot{z}(t)+\rho gSz(t)+k_l z(t)+k_n z^3(t)=f_{dzregular}$$
$$\dot{\mathbf{X}}(t)=\mathbf{A}^{'}\mathbf{X}(t)+\mathbf{B}^{'}\dot{z}(t) \tag{16}$$

$$[m+A_z(\infty)]\ddot{z}(t)+\mathbf{C}'\mathbf{X}(t)+C\dot{z}(t)+\rho gSz(t)+k_l z(t)=f_{dzregular}$$
$$\dot{\mathbf{X}}(t)=\mathbf{A}^{'}\mathbf{X}(t)+\mathbf{B}^{'}\dot{z}(t) \tag{17}$$

The function (16) and (17) are calculated using Runge-Kutta method by MATLAB. We assumed that the initial conditions is $\boldsymbol{\lambda}=[0 \quad \cdots \quad 0]^{T}_{7\times 1}$.

The time-averaged power capture of PTO system can be calculated

$$P=\frac{1}{T_2-T_1}\int_{T_1}^{T_2}C\dot{z}^2dt \tag{18}$$

The power ratio is defined as

$$C_p=\frac{P}{P_0} \tag{19}$$

where, $P_0$is time-averaged power capture of linear PTO system.

IV. RESULTS AND DISCUSS

Through (13) and (14), the resonance angular frequency and the optimum damping coefficient can be obtained, i.e. $\omega_0=1.4058$ rad/s and $C_{opt}=64652$ N/(m/s). The nonlinear parameter α ($\alpha=k_n/k_l$) is chosen from 0 to 1 for research the nonlinear WEC. About the JONSWAP wave spectrum, $H_s=2$ m and $\gamma=3$ are adopted in this paper. When $\omega_m=1$ rad/s, the power spectrum density and the wave height of JONSWAP wave are obtained as shown in Figure 5.

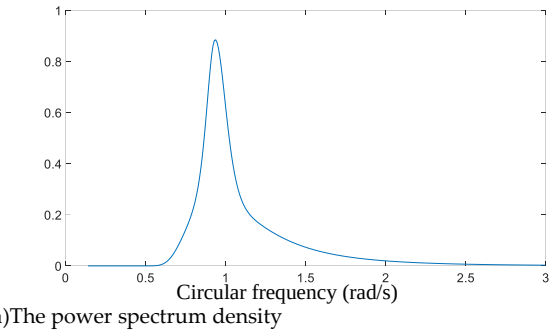

(a)The power spectrum density

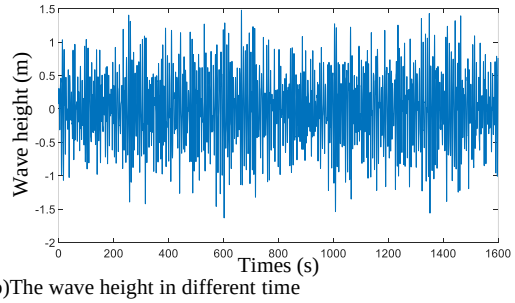

(b)The wave height in different time

Fig. 5. The irregular waves (JONSWAP wave spectrum:$H_s=2m$, $\gamma=3$ and $\omega_m=1rad/s$)

The averaged power capture of WEC can be calculated by calculated from 2000 s to 4000 s using (18) considering the different significant wave heights. The power ratio of WEC is also analyzed. The results are shown in Figure 6. From Figure 6, the captured energy of WEC increases following the significant wave height increasing. When the peak frequency is close to the natural frequency of the PA-WEC system (1.4 rad/s), the captured energy of nonlinear WEC reduces following the nonlinear parameters increasing. With the significant wave heights and nonlinear parameters increasing, the decreasing trend of captured energy becomes more obvious. When the peak frequency is larger than 1.67 rad/s, the captured energy of system can obtained more energy than the linear WEC.

Considering different peak frequencies and nonlinear parameters, the averaged power capture of WEC is calculated in different significant wave heights as shown in Figure 7. From Figure 7, the power increases along with the significant wave height increasing. And the change of power is not obvious with the nonlinear parameter increasing. However, if the peak frequency is less than the natural frequency, the power ratio decreases with significant wave heights and nonlinear parameters increasing. When the peak frequency is $\omega_m=2.1$ rad/s, the power ratio increases with significant wave height and nonlinear parameter increasing.

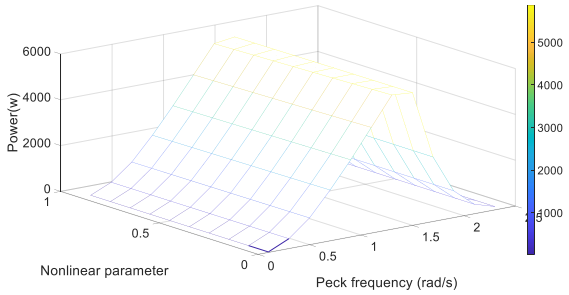

(a) $H_s = 1$ m

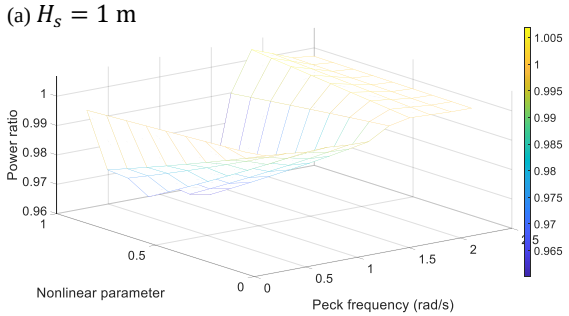

(b) $H_s = 1$ m

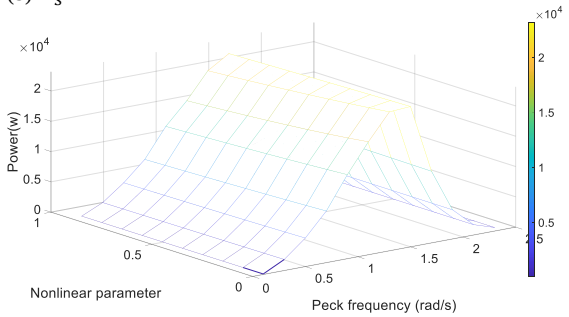

(c) $H_s = 2$ m

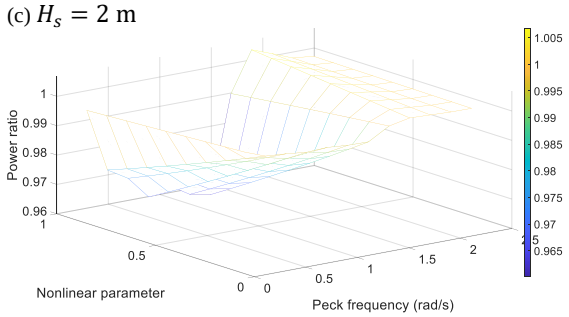

(d) $H_s = 2$ m

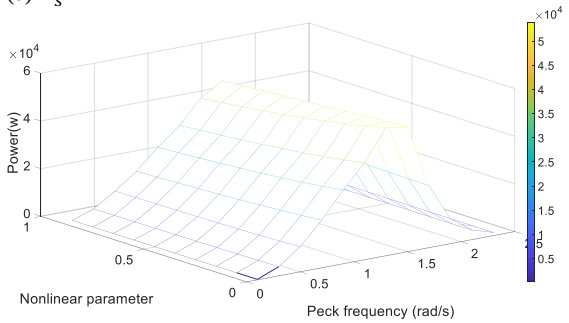

(e) $H_s = 3\ m$

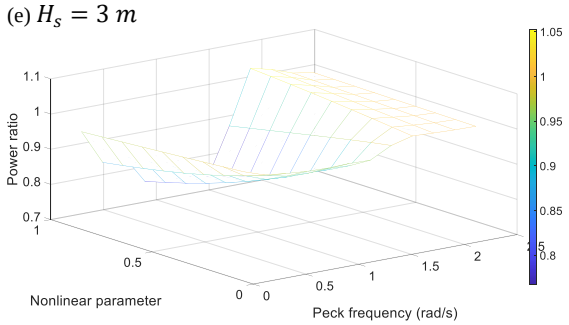

(f) $H_s = 3$ m

Fig. 6. The power and power ratio of WEC in different peak frequencies and nonlinear parameters with the different significant wave heights (a) (b) $H_s = 1$ m ; (c) (d) $H_s = 2$ m ; (e) (f) $H_s = 3$ m .

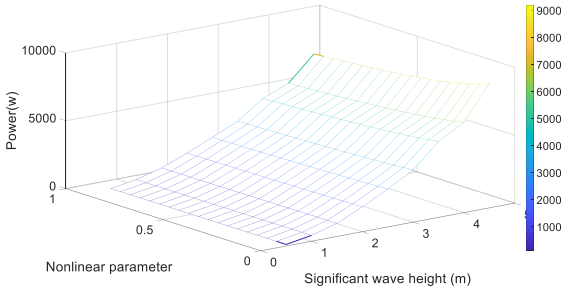

(a) $\omega_m = 0.3$ rad/s

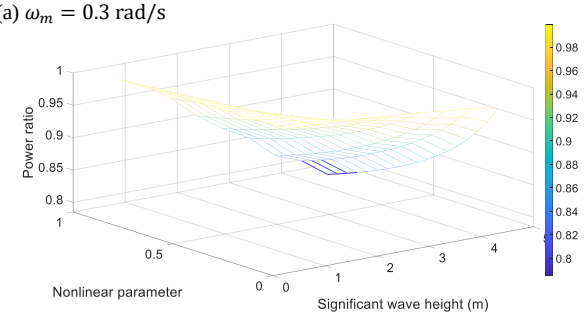

(b) $\omega_m = 0.3$ rad/s

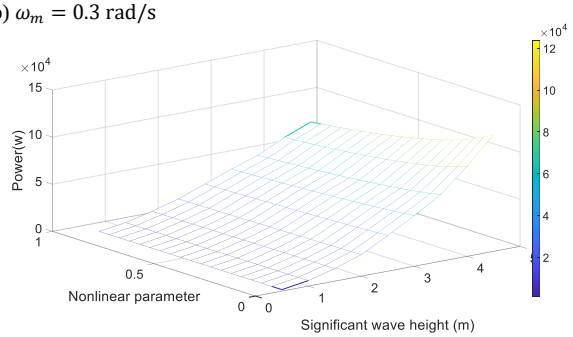

(c) $\omega_m = 1.3$ rad/s

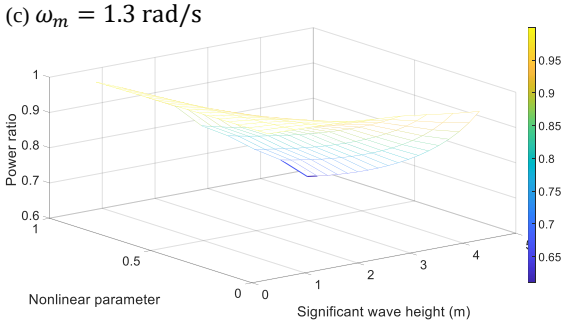

(d) $\omega_m = 1.3$ rad/s

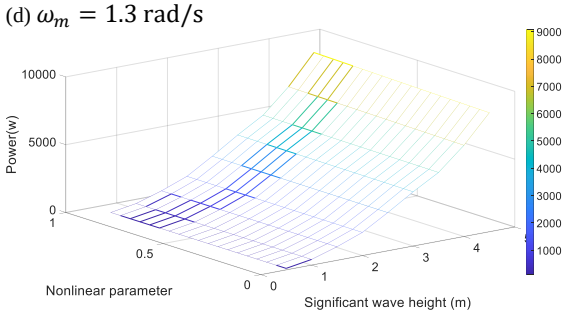

(e) ω_m=2.1 rad/s

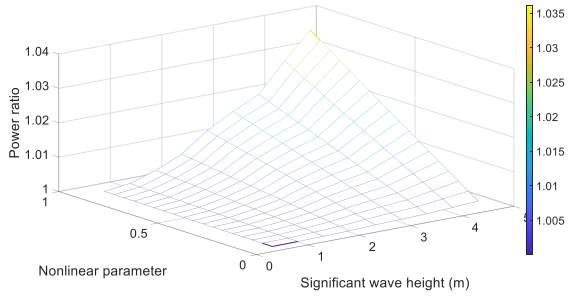

(f) ω_m=2.1rad/s

Fig. 7. The power and power ratio of WEC in different significant wave heights and nonlinear parameters with the different peak frequencies (a) (b) $\omega_m = 0.3rad/s$; (c) (d) $\omega_m = 1.3rad/s$; (e) (f) ω_m=2.1rad/s .

The value of damping parameter $\beta = \frac{C}{C_{opt}}$ is in range [0.5, 1.5]. The effect of power of WEC is simulated with different damping parameters and peak frequencies in different nonlinear parameters. The results are shown in Figure 8. Though increasing the damping, the captured energy will increase. And the damping has a little effect to the peak frequency. However, the nonlinear parameter almost has nothing effect to the power ratio.

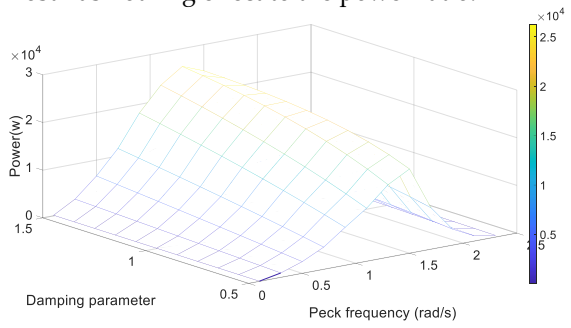

(a) $\alpha = 0.1$

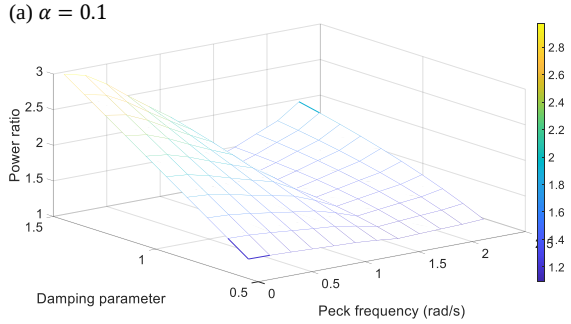

(b) $\alpha = 0.1$

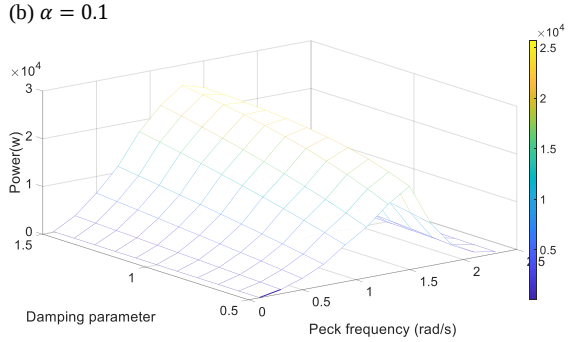

(c) $\alpha = 0.3$

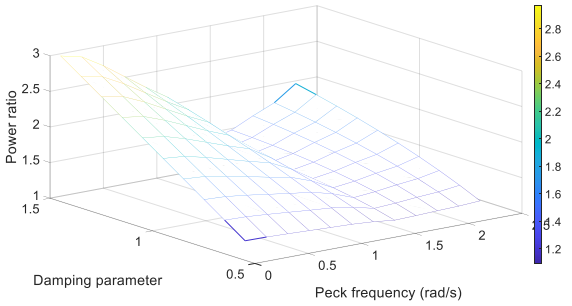

(d) $\alpha = 0.3$

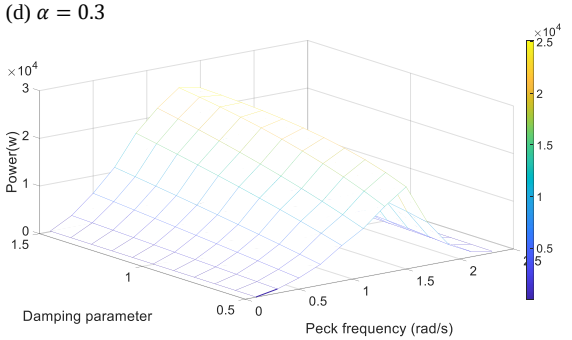

(e) $\alpha = 0.5$

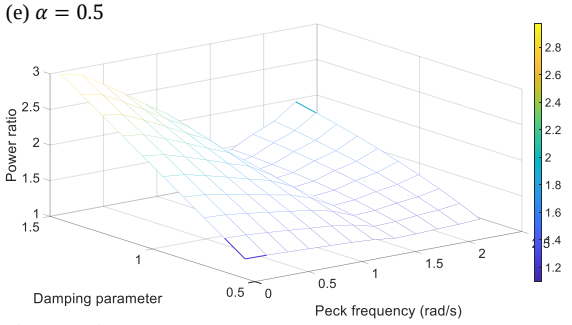

(f) $\alpha = 0.5$

Fig. 8. The power and power ratio of WEC in different peak frequencies and damping parameter with the different nonlinear parameters (a) (b) $\alpha = 0.1$; (c) (d) $\alpha = 0.3$; (e) (f) $\alpha = 0.5$.

V. CONCLUSION

This paper studies the dynamic response of a PA-WEC with nonlinear hardening spring PTO systems under irregular waves. The time domain method is developed the dynamic model of WEC considering the JONSWAP wave spectrum. The results are calculated by MATLAB with state space model. For the larger motion, the nonlinear parameter increasing will lead to the captured energy of the WEC decreasing. When the peak frequency is close to the natural frequency of the PA-WEC system (1.4rad/s), the system has maximum power captured. The significant wave height will increase the power capture but the effect of nonlinear parameter become more obvious. The damping parameter increasing can lead to the power capture of WEC increasing.

REFERENCES

[1] A. F. de O Falco, "Wave energy utilization: A review of the technologies", *Renewable and Sustainable Energy Reviews*, vol. 14, no. 3, pp. 899-918, 2010.DOI: doi.org/10.1016/j.rser.2009.11.003.

[2] B. Drew, A. R. Plummer, and M. N. Sahinkaya, ”A review of wave energy converter technology”, *Proceedings of the Institution of Mechanical Engineers, Part A: Journal of Power and Energy*, vol.

223, no. 8, pp. 887-902, 2009.DOI: doi.org/10.1243/09576509JPE782.

[3] P. C. Vicente, A. F. de O Falco, and P. A. Justino, "Nonlinear dynamics of a tightly moored point-absorber wave energy converter", *Ocean engineering*, vol. 59,pp. 20-36, 2013.DOI: doi.org/10.1016/j.oceaneng.2012.12.008.

[4] R. Crozier, H. Bailey, M. Mueller, E. Spooner, and P. McKeever," Analysis, design and testing of a novel direct-drive wave energy converter system". *IET Renewable Power Generation*, vol. 7, no. 5, pp. 565-573, 2013.DOI: 10.1049/iet-rpg.2012.0072.

[5] H. Bailey, and I. Bryden, "Nonlinear Modelling of Power Take Off Systems". *In OCEANS 2007-Europe* , 2007.

[6] X. Zhang, and J. Yang, "Power capture performance of an oscillating-body WEC with nonlinear snap through PTO systems in irregular waves", *Applied Ocean Research*, vol. 52, pp. 261-273, 2015.DOI: 10.1016/j.apor.2015.06.012.

[7] K. Tarrant, and C. Meskell, "Investigation on parametrically excited motions of point absorbers in regular waves", *Ocean Engineering*, vol. 111, pp. 67-81, 2016.DOI: 10.1016/j.oceaneng.2015.10.041

[8] B. P. Mann, and N. D. Sims, "Energy harvesting from the nonlinear oscillations of magnetic levitation", *Journal of sound and vibration*, vol. 319, no. 1-2, pp. 515-530, 2009. DOI: 10.1016/j.jsv.2008.06.011.

[9] S. P. Pellegrini, N. Tolou, M. Schenk, and J. L. Herder, "Bistable vibration energy harvesters: a review", *Journal of Intelligent Material Systems and Structures*, vol. 24, no. 11, pp. 1303-1312, 2013, DOI: 10.1177/1045389x12444940.

[10] Z. Liu, "A nonlinear double-speed electromagnetic vibration energy harvester for ocean wave energy conversion", Doctoral dissertation, RMIT University, 2017.

[11] D. G. Wilson, G. Bacelli, R. Robinett III, and O. Abdelkhalik, "Nonlinear Control Design for Nonlinear Wave Energy Converters ", Sandia National Lab.(SNL-NM), Albuquerque, NM (United States), 2018.

[12] S. Sun, X. Dai, K. Wang, X. Xiang, G. Ding, and X. Zhao, "Nonlinear electromagnetic vibration energy harvester with closed magnetic circuit", *IEEE Magnetics Letters*, vol. 9, pp. 1-4, 2018, DOI: 10.1109/LMAG.2018.2822625.

[13] D. G. Wilson, R. D. Robinett, G. Bacelli, O. Abdelkhalik, and R. G. Coe, "Extending Complex Conjugate Control to Nonlinear Wave Energy Converters", *Journal of Marine Science and Engineering*, vol. 8, no. 2, pp. 84, 2020, DOI: 10.3390/jmse8020084.

[14] Z. Wu, C. Levi, and S. F. Estefen, "Wave energy harvesting using nonlinear stiffness system", *Applied Ocean Research*, vol. 74, pp. 102-116, 2018, DOI: 10.1016/j.apor.2018.02.009.

[15] T. D. Dang, M. N. Nguyen, and K. K. Ahn, "A Study on Wave Energy Converter with Variable Stiffness Mechanism", *In 2019 23rd International Conference on Mechatronics Technology (ICMT)* ,pp. 1-5,2019.

[16] Z., Zheng, Z. Yao, Z. Chang, T. Yao, and B. Liu, "A point absorber wave energy converter with nonlinear hardening spring power-take-off systems in regular waves", *Proceedings of the Institution of Mechanical Engineers, Part M: Journal of Engineering for the Maritime Environment*, vol. 234, no. 4, pp. 820-829, 2020, DOI: 10.1177/1475090220913687.

[17] A. de la Villa Jaén, D. E. M. Andrade, and A. Garcia Santana, "Increasing the efficiency of the passive loading strategy for wave energy conversion", *Journal of Renewable and Sustainable Energy*, vol. 5, no. 5, pp. 053132, 2013.DOI: 10.1063/1.4824416.

[18] A. Babarit, and A. H. Clément, "Optimal latching control of a wave energy device in regular and irregular waves", *Applied Ocean Research*, vol. 28, no. 2, pp. 77-91, 2006, DOI: 10.1016/j.apor.2006.05.002.

[19] J. Sjolte, C. M. Sandvik, E. Tedeschi, and M. Molinas, "Exploring the potential for increased production from the wave energy converter lifesaver by reactive control", *Energies*, vol. 6, no. 8, pp. 3706-3733, 2013, DOI: 10.3390/en6083706.

[20] A. Babarit, M. Guglielmi, and A. H. Clément, "Declutching control of a wave energy converter", *Ocean Engineering*, vol. 36, no. 12-13, pp. 1015-1024, 2009, DOI: 10.1016/j.oceaneng.2009.05.006.

[21] J. A. Cretel, G. Lightbody, G. P. Thomas, and A. W. Lewis, "Maximisation of energy capture by a wave-energy point absorber using model predictive control", *IFAC Proceedings Volumes*, vol. 44, no. 1, pp. 3714-3721, 2011, DOI: 10.3182/20110828-6-it-1002.03255.

[22] U. A. Korde, "On a near-optimal control approach for a wave energy converter in irregular waves", *Applied Ocean Research*, vol. 46, pp. 79-93, 2014, DOI: 10.1016/j.apor.2014.02.002.

[23] M. Richter, M. E. Magana, O. Sawodny, and T. K. Brekken, "Nonlinear model predictive control of a point absorber wave energy converter", *IEEE Transactions on Sustainable Energy*, vol. 4, no. 1, pp. 118-126, 2012, DOI: 10.1109/TSTE.2012.2202929.

[24] Y. A. Goda, "Comparative Review on the Functional Forms of Directional Wave Spectrum", *Coastal Engineering Journal*, vol. 41, no. 1, pp. 1-20, 1999, DOI: 10.1142/S0578563499000024.

[25] W. E. Cummins, "The impulse response function and ship motions", *Schiffstechnik*, vol. 9, pp. 101-109, 1962.

[26] R. Taghipour, T. Perez, and T. Moan, "Hybrid frequency–time domain models for dynamic response analysis of marine structures", *Ocean Engineering*, vol. 35, no. 7, pp. 685-705, 2008, DOI: 10.1016/j.oceaneng.2007.11.002.

[27] T. Pérez, and T. I. Fossen, "Time-vs. frequency-domain identification of parametric radiation force models for marine structures at zero speed", *Modeling, Identification and Control*, vol. 29, no. 1, pp. 1-19, 2008, DOI: 10.4173/mic.2008.1.1.